



# Firefighting of subsurface coal fires with comprehensive techniques for detection and control: a case study of the Fukang coal fire in the Xinjiang region of China

Bo Tan<sup>1</sup> · Feichao Zhang<sup>1</sup> · Qingsong Zhang<sup>2</sup> · Hongyi Wei<sup>1</sup> · Zhuangzhuang Shao<sup>1</sup>

Received: 26 April 2019 / Accepted: 29 July 2019 / Published online: 17 August 2019  
© Springer-Verlag GmbH Germany, part of Springer Nature 2019

## Abstract

Coal fires are global disasters, and China suffers the most serious coal fire disasters in the world. This paper introduces detailed detection and extinguishing methods for the wide range and complex coal fires at the No. 1 well in the Fukang mining area. First, the characteristics of the large and complex coal fire areas in the No. 1 well in the Fukang mining area are introduced, and 5 large fire areas are detected using the comprehensive detection range method, which detects fire areas before fire engineering practices are implemented. From the characteristics of this large-scale, complex coal fire, the zonal fire extinguishing scheme is formulated, designed, and applied, and the “shallow open fire stripping—construction of the boundary isolation zone—drilling and grouting in the deep fire area” series of events is utilized in the zonal fire extinguishing scheme. A new type of sodium silicate gel in compressive moisturizing plastic packing materials is used, an automatic grouting system is developed, and effective grouting processes are proposed, which can be adjusted according to the grouting effect analysis of the grouting parameters to determine the natural sedimentation and diffusion radius. After the construction was completed, the fire extinguishing effect was tested, revealing that the temperature in the fire zone cooled in a short time, and no subsequent heating phenomenon occurs. The method proposed in this paper provides guidance and a reference for other coal fires in the world.

**Keywords** Large-scale complex coal fire · Zonal fire extinguishing scheme · Outcrop coal fire · Hidden fire · Filling material

---

Responsible editor: Philippe Garrigues

---

✉ Bo Tan  
tanbo709@126.com

Feichao Zhang  
zhangfeichao81@163.com

Qingsong Zhang  
375012563@qq.com

Hongyi Wei  
842283416@qq.com

Zhuangzhuang Shao  
1003882864@qq.com

<sup>1</sup> Faculty of Emergency Management and Safety Engineering, China University of Mining & Technology (Beijing), Beijing, China

<sup>2</sup> China Coal Technology Engineering Group, Chongqing Research Institute, Chongqing, China

## Introduction

Coal field fires refer to large-scale fires that occur in the outcrop or shallow part of a coal seam, and these fires affect the development of coal fields, destroy valuable resources, seriously contaminate the environment, and pose a threat to production safety (Stracher 2004; Zhang 2008). Among all the countries, China suffers the most serious coal fire disasters in the world (Kong et al. 2017; Stracher et al. 2013). According to incomplete statistical data, 20 million tons of coal are burned annually in coal fires in China (equivalent to Turkey's total coal output of 20.8 million tons in 2017 (BP 2018)), and nearly ten times this amount of coal resources are affected (Dijk et al. 2011). Coal fire disasters not only waste a large amount of precious coal resources but also cause environmental pollution, property damage, and other hazards. The direct combustion of untreated coal not only generates a large amount of greenhouse gases (CO<sub>2</sub> and CH<sub>4</sub>) (Kuenzer and Stracher 2012; Kuenzer et al. 2007) but also emits large amounts of toxic gases (CO, SO<sub>2</sub>, H<sub>2</sub>S, and NO<sub>x</sub>) and toxic elements (As, F, S, Hg), damaging the local ecological

environment and posing a threat to personnel safety (Finkelman 2004; Liang et al. 2014; Song et al. 2014).

Coal fires in China are mainly distributed along the northern latitude from 36° to 45°, and Xinjiang is located along this strip (Song and Kuenzer 2014). The coal fire distribution in Xinjiang is shown in Fig. 1(b). According to the coal-forming period, China’s coal can be divided into five distribution regions, as shown in Fig. 1(a). Xinjiang is located in the northwest coal-producing region, and the coal in this region was formed during the early and middle Jurassic periods; the coal formed during this period has a high tendency for spontaneous combustion due to its low rank and abundant oxygen-containing functional groups and volatile components (Li et al. 2016; Song and Kuenzer 2014; Wang 2013). In addition, the dry climate, low rainfall amount (less than 500 mm/a) (Cao and Shi 2009), shallow burial, and large number of outcrops of coal seams in Xinjiang all provide suitable natural conditions for spontaneous coal combustion (Song et al. 2019).

The accurate detection and location of underground coal fires are key to fire extinguishing engineering practices. Xue et al. (2008) conducted two field tests on an underground coal fire in Australia using <sup>222</sup>Rn technology. The results showed that the heating depth of underground coal reached 450 m, and an isolated <sup>222</sup>Rn anomaly was generated on the surface above the vertical heating belt. The underground coal fire locations can be delineated by monitoring the abnormal radon concentration on the surface. The disadvantage of this

method is that local coal fires are buried at a greater depth, meaning that radon gas released by radon sources cannot reach the surface directly. Using the fifth fire area as an example, Shao et al. (2018) adopted the magnetic potential and the self-potential methods to determine the fire scope and, on the basis of the two methods, proposed a composite index, which can combine the advantages of the two methods and provide a comprehensive response to both shallow and deep fires. Song (Song and Kuenzer 2017; Song et al. 2015) extracted Landsat data using an automated moving-window thermal anomaly extractor, analyzed the Wuda fire area in China, and combined the information with an on-site investigation of Wuda coal fires. The thermal anomaly extractor proved to be effective for thermal anomaly extraction and provided an efficient method for large-area fire detection.

For fire extinguishing technology in coal mines, scholars have proposed a comprehensive fire extinguishing method based on the combination of inert gas, cooling and new fire extinguishing materials, resulting in the rapid development of coal mine fire prevention technology. Shao et al. (2015) combined three-phase foam technology with a water-mist fire extinguishing system and integrated the advantages of the two methods for practical applications at an open coal mine site, effectively controlling underground fires and ensuring the safety of personnel and equipment. This method can provide a valuable method of fire control for upper fires in loose zones and abandoned roadways. Liu et al. (2018) applied dry ice for underground firefighting and developed a new device for

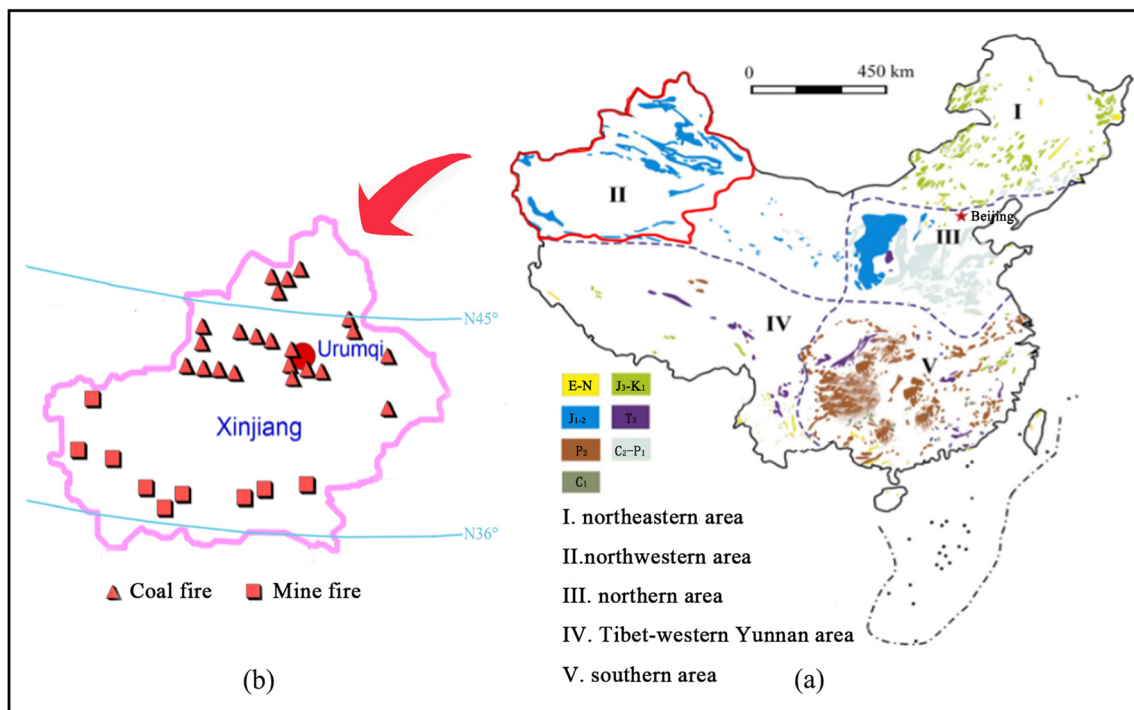


**Fig. 1** China’s coal and Xinjiang’s coal fire distribution map. (a) China’s coal distribution map (Dai et al. 2012), in which coal in Xinjiang basically formed in the early and middle Jurassic period. (b) Coal fire distribution in Xinjiang (Zeng et al. 2015) along the northern latitude from 36° to 45°

high-efficiency sublimation of dry ice. The amount of carbon dioxide generated by dry ice using high-efficiency sublimation is 205 times higher than that generated by dry ice under normal circumstances. This was also the case in the China Yangquan No. 5 Coal Mine, thus achieving good results. Injection of carbon dioxide from rapidly sublimating dry ice is a high-performance approach for fighting the early, spontaneous combustion of coal underground due to its cooling and inertia effects. Compared with water injection, this approach does not deteriorate the working environment, thereby improving the work efficiency. Rúa et al. (2018) evaluated the coal mine fire situation at the Cerrejón mine and developed diluted bitumen and brine (a combustion inhibitor), cement/slaked lime, fine sand cement, and clinker/slaked lime to avoid ignition. The field results showed that the asphalt/brine had good adhesion and durability in the coal seam. This method is an economical and efficient underground fire extinguishing scheme.

The coal fires in the No. 1 well of the Fukang mining area are complex; the burial depth and burning degree of various fire zones are different. Each fire source detection method has its own advantages, disadvantages, and ranges of use, and the application of a single detection method is not enough to detect and locate the entire fire area. In addition, the mine has a large area of cavity caused by the fire zone and cracks caused by the collapse of the ground. The measures of only grouting and plugging are no longer enough. The existing grouting technology has the disadvantages of large water consumption and low-strength grouting materials. Besides, a single grouting parameter for the grouting process cannot guarantee the natural precipitation and diffusion radius of a slurry in complex fire areas.

Therefore, the purpose of this study is twofold. The first purpose is to use a variety of detection methods to accurately detect complex coal fire areas and introduce the detection and extinguishing methods for a large complex coal fire area. The second purpose is to develop a new type of sodium silicate gel for use as a compressive moisturizing plastic packing material that can resist pressure and retain moisture and to develop an automatic grouting system to introduce a set of effective grouting processes that can improve the effectiveness of grouting.

## Overview of the Fukang coal fire in Xinjiang, China

The No. 1 well of the Fukang mining area is located 13 km southeast of Fukang City, Xinjiang Autonomous Region, as shown in Fig. 2. At present, at the No. 1 well, there are three minable coal seams, A2, A3, and A4, with top-down ordinal numbers for A2, A3, and A4; the dip angle of the coal seams is approximately 23°. A2 is the most minable coal seam in this

mining field, where the average minable coal seam thickness is 9.84 m. The average minable coal seam thicknesses of the A3 and A4 coal seams are 2.09 m and 2.22 m, respectively, and their structures are simple.

There are 8 original production mines and old kilns in the well field, and all of them had been closed by July 2005. From 2008 to 2009, during the renovation of the mine, there were many gas explosion accidents during the process of fire control. After the closure of the Shenlong coal mine, which was the original production mine, many high-temperature danger areas remained.

Generally, the fire intensity was strong in the west and weak in the east, and most of the A2 coal seam was burnt. A3 and A4 coal seams were subjected to different degrees of fire at the shallow part of the surface and there was sporadic fire in the deep. From the process of mine exploitation and fire control, we can see that there are two major problems, one is that after coal seam being subjected to different degrees of fire, high-temperature cavity is formed, which causes surface collapse and air leakage, and oxygen supply increases, aggravating coal seam combustion. On the other hand, the distribution location of small coal mine goaf that formed in history is not clear and there was a large amount of residual coal, which will also increase the difficulty of fire control.

## Firefighting scheme using comprehensive techniques

It is impossible to apply a single detection scheme or fire extinguishing scheme because of the site conditions of the large-scale complex coal fire. Therefore, comprehensive detection and fire extinguishing schemes should be developed according to the characteristics of each fire area and local conditions.

Due to the large scope of the fire area, the fire area has the characteristics of seam outcrops, small coal pits, and deep mine fires; thus, the overall fire area detection scheme of the “infrared detection of shallow outcrop fire—isotope radon detection of hidden fire area—drilling and temperature measurement verification” series was formulated. Since the depth of the shallow surface outcrop fire is buried, the surface heat release phenomenon is obvious, and the outcrop fire source area and the development degree of the fire can be directly determined by a YRH310 infrared thermal imager. According to the trends of outcrop fires extending along the coal seam, temperature measurements and sampling analysis of boreholes are used for the outcrop fire area. For hidden fire sources in deep coal mines, it is impossible to judge the fire source range directly by index gas collection and temperature indices in the underground area due to the lack of geological production data. The isotope method using radon detection on the surface of the high-temperature

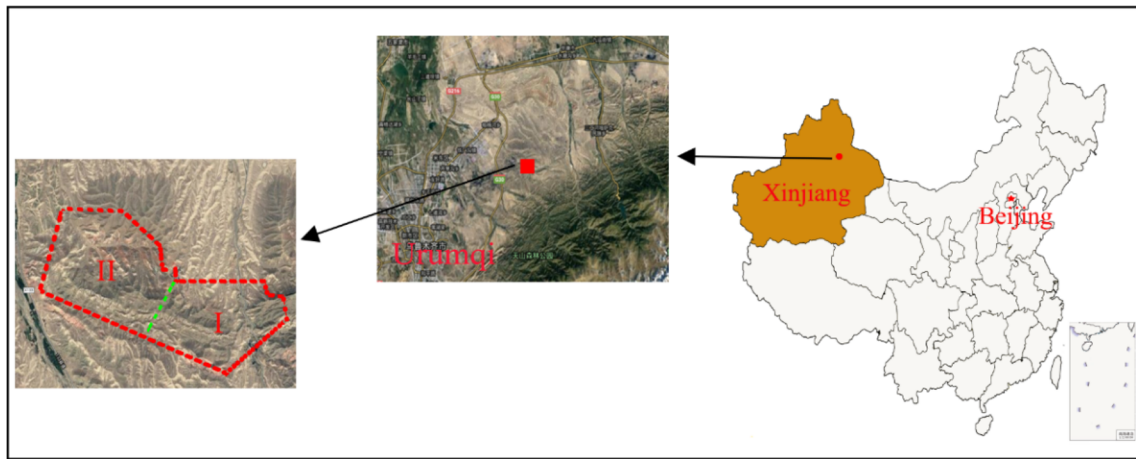


**Fig. 2** The location of the No. 1 well in the Fukang mining area in China. The data on the left and in the middle are collected from Google Maps in 2018. (I) and (II) in the left picture represent the first and second sections, respectively

area underground can be applied. In the process of fire area detection, the active RAD7-type continuous radon measuring instrument was applied, and the average concentration of radon was measured using continuous monitoring, which is more accurate and reliable than other radon measuring technologies. Based on the preliminary judgment of a wide range of fire sources using the isotope measurement of radon technique, the surface drilling method is adopted to monitor the temperature and gas in the borehole and further judge the high-temperature fire source point and fire area in the mine goaf. A borehole temperature measuring device adopts armored thermocouple measurements, and the highest monitoring temperature is up to 1000 °C.

Due to the complicated types of coal fire in this fire area, it is necessary to conduct a comprehensive analysis of the investigation and drilling results at the fire area during its treatment and adopt the overall technical scheme of “shallow open fire stripping—construction of the boundary isolation zone—drilling and grouting in the deep fire area.” As shown in Fig. 3, in the outcrop fire area of the coal seam, the loose outcrop naked fire mainly peels off, and then the air leakage and oxygen supply at the high-temperature fire source point are reduced by the grouting and loess coverage to achieve fire suppression. For the fire zone boundary, to prevent the fire from spreading to the unburned zone, an isolation zone will be built at the fire zone boundary to separate the high-temperature burning zone from the unburned zone. According to the dynamic monitoring results in the fire area, different filling and grouting materials were selected, and the isolation parameters were dynamically adjusted. For large-area fire control in nonboundary areas, firefighting is mainly carried out by pouring different proportions of yellow mud mixed with JTJ-1 colloidal material into the deep borehole above the fire area. In the process of grouting, the grouting material and parameters are dynamically adjusted according to the dynamic monitoring results in the fire area.

The fire control area of this construction is large, and the construction period is long, so the project is divided into two stages; the area of the first section is 162,000 m<sup>2</sup>, and the area of the second section is 302,000 m<sup>2</sup>, as shown on the left in Fig. 2.

### Subsurface fire detection

Infrared thermal imaging can measure the surface temperature accurately, but it cannot detect the deep-buried fire area; however, the radon measuring technology compensates for this because it can theoretically provide direct exploration. However, due to the large area of shallow buried coal seams in the Fukang coal mine, the time and expense the overall arrangement of measuring radon in coal seams are greatly increased. Infrared thermal imaging technology controls the detection range well. To determine the fire source range accurately and guide the subsequent firefighting work, the infrared camera-assisted radon measurement method is adopted to detect the fire area.

### Shallow deep coal fire detection

There are coal outcrops of different degrees in the A2 coal seam of the No. 1 well in the Fukang mining area. High-temperature positions can be detected using infrared thermal imaging, as the outcrop coal has a relatively shallow burial. Infrared detection technology is based on infrared radiation principles for measuring the temperature or radiation energy of the object. In nature, any object emits infrared electromagnetic waves if the temperature is above absolute zero (− 273 °C); thus, an infrared radiation field is formed. The radiation energy is as follows (1):

$$E = \varepsilon\sigma T^4 \tag{1}$$

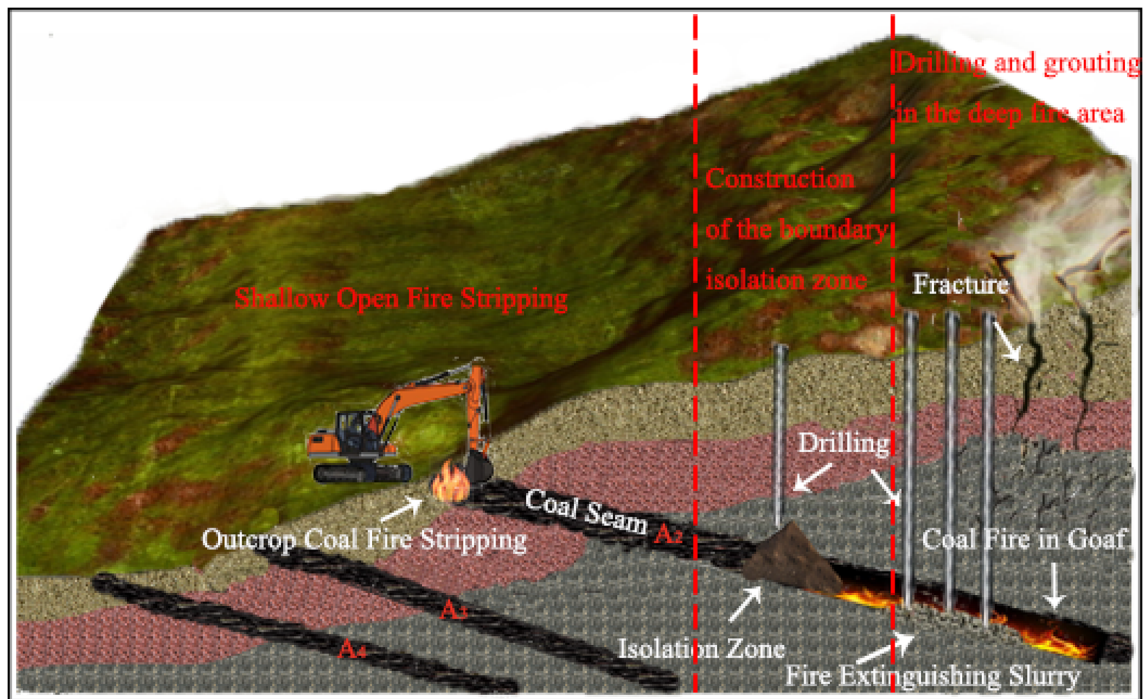


**Fig. 3** Schematic diagram of the fire extinguishing scheme in the fire area; stripping of the open fire is adopted to deal with the outcrop fire area. Building a separating wall to prevent the spreading of fire and the methods of drilling and grouting are used to extinguish fires in the deep fire area

where  $E$  is the radiant flux density,  $W/m^2$ ;  $\varepsilon$  is the radiation rate on the surface of a body, which is determined only by the surface properties of the body; here,  $0 < \varepsilon < 1$  and has values of approximately 0.8–0.98 for rocks and coal bodies;  $\sigma$  is the Stephen-Boltzmann constant,  $\sigma = 5.67 \times 10^{-8} W/(m^2 * K^4)$ ; and  $T$  is the surface temperature of the radiation unit, K.

As seen from the above equation, for the same object, the higher the temperature is, the greater the radiation energy, and the stronger the radiation energy field. The cavities generated by the spontaneous combustion of the coal seam form cracks and collapse pits on the surface, the heat generated by the spontaneous combustion will spread to the air along the outcrop of the coal seam and surface cracks, and the surface temperature is monitored by infrared thermal imaging.

Infrared thermal imaging was used to obtain an omnidirectional and multiangle infrared photograph of the No. 1 well in the Fukang mining area. According to the infrared detection results, 6 high-temperature areas were found. At that time, the average outdoor temperature was 5 °C, and 6 locations were found to be over 30 °C. These locations are named A, B, C, D, E, and F.

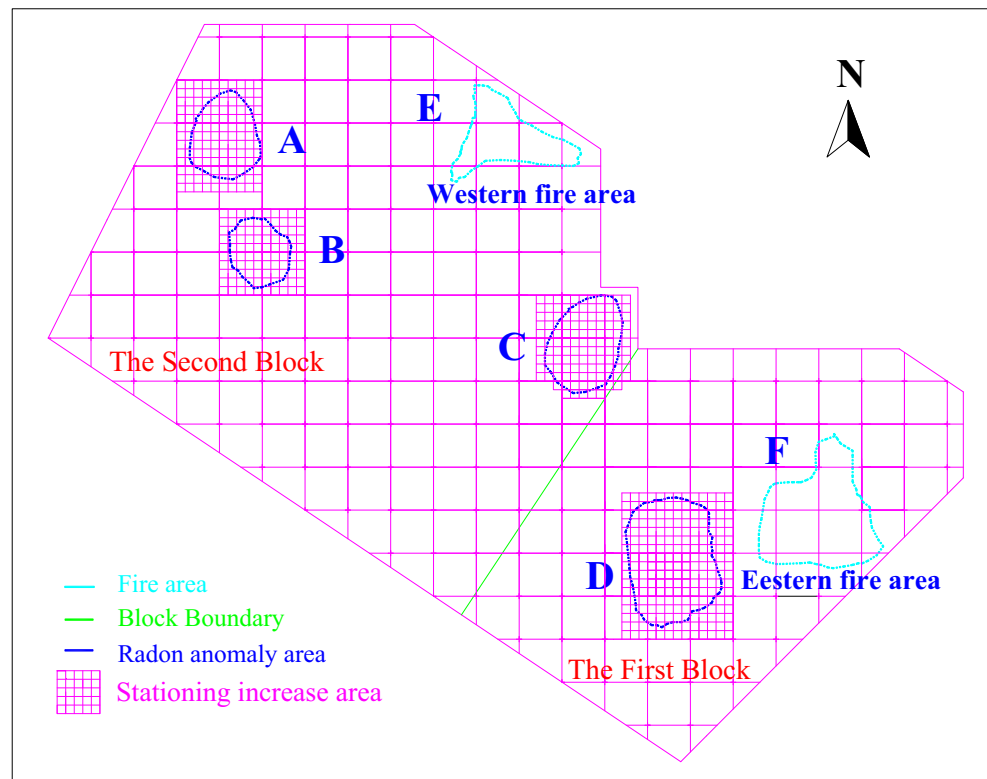
The shallow coal seam is located near the crustal surface and is affected by seasonal and climatic changes. Under the long-term action of thermal stress, the coal seam is seriously eroded by weathering erosion and has a loose structure and large porosity. A large number of free surfaces are produced by the surface fragmentation of coal, which allows air currents caused by temperature differences to penetrate. As the

temperature of coal increases, the hot air pressure, the intensity of air leakage, and the rate of oxygen consumption increase gradually. High temperatures form when shallow coal fires burn, and the air density near the outcrop of the coal seam is higher than that in the lower goaf, forming the fire wind pressure. Due to the action of the upward force of the fire wind pressure, an updraft is formed, and the gas in the lower goaf continuously supplies oxygen to the high-temperature coal in the upward part.

The maximum temperatures of E and F in the 6 high-temperature regions reached 77.2 °C and 52.7 °C, respectively (as shown in Fig. 4). If the normal heat flow and the radiation background caused by the solar radiation variation on Sunday are not taken into account, it can be assumed that the amount of thermal radiation obtained from the surface mainly depends on the heat transferred from the underground coal seam to the surface, and there is a close correspondence between the two. Therefore, combining Fig. 4 and the geological map of the coal seam, it can be concluded that the E and F fire zones are the west burning area and the east burning area of the outcrop of the A2 coal seam, respectively.

Figure 5(a) is the infrared thermal image obtained in the east burning area of the outcrop of the A2 coal seam, in which the white area is the high-temperature area, and the highest regional temperature shown in this figure is 52.7 °C. In the field in Fig. 5(b), the high-temperature area is circled according to infrared thermal imaging. Similarly, according to Fig. 6(a), the highest regional temperature in the west burning area of the outcrop of the A2 coal seam is 77.2 °C; in Fig. 6(b), the

**Fig. 4** Relative locations of the two surface fire zones and four high-temperature zones determined by infrared thermal imaging



high-temperature area is circled. The total area of the two outcrop fire areas is approximately 21,500 m<sup>2</sup>.

**Concealed fire source detection**

Since infrared thermal imaging can only measure the surface temperature of the object, the corresponding vertical points in the high-temperature area monitored from the surface are not necessarily the real high-temperature fire sources. Therefore, when determining concealed fire source locations in the No. 1 well in the Fukang mining area, on the basis of infrared thermal imaging, the deep fire area should be detected using isotopic radon measurements and verified by surface borehole temperature measurements.

1. The radon method is used to detect concealed fire sources

The principle of the isotopic radon method for detecting fire zones is as follows: under the same geological stratum conditions, when the local lower coal seam is heated by oxidation or spontaneous combustion, the natural radioactive radon exhalation rate increases in the surrounding and overlying strata, and radioactive anomalies are formed on the surface, which can be detected to reflect temperature information.

For the field detection process, a GPS locator is first used to locate and select the datum point of the measurement field. According to the accuracy requirements of the field, as shown in Fig. 4, a 50-m x 50-m grid spacing is adopted for the later-type detection, and 205 detection points are used. When six high-temperature regions were detected by infrared thermal

**Fig. 5** Determination of high-temperature points in the east burning area of the outcrop of the A2 coal seam by infrared thermal imaging

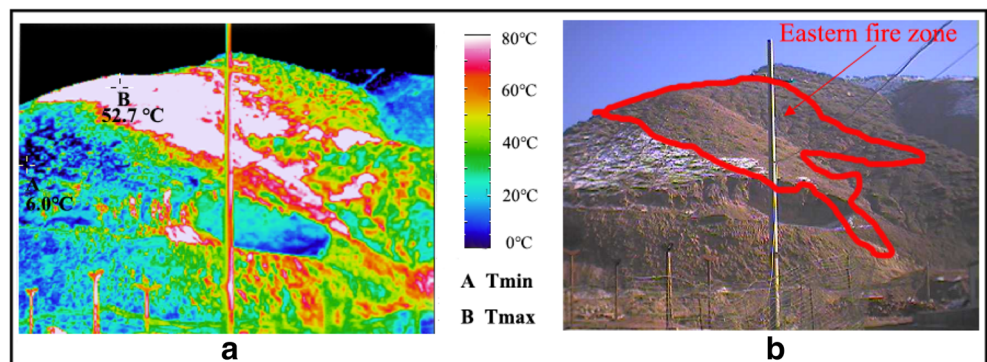
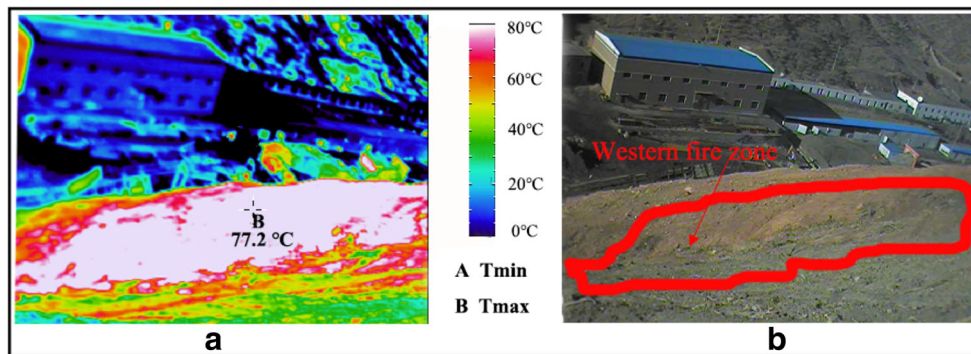


**Fig. 6** Determination of high-temperature points in the west burning area of the outcrop of the A2 coal seam by infrared thermal imaging



imaging, the detection interval was adjusted to 10 m × 10 m, as shown in Fig. 4; 601 detection points were added on the original basis, and the boundary of the abnormal region with radon values was determined through the layout of the encrypted detection points.

The field measurement data were input into the data processing system for radon detection, and the analysis showed that the maximum radon concentration was one of the abnormal radon emission points. The maximum radon concentration was 31,551.09 Bq/m<sup>3</sup>, the average radon concentration was 7,223.495 Bq/m<sup>3</sup>, the median radon concentration was 6,107.177 Bq/m<sup>3</sup>, and the ratio of the maximum value to the median value was 5.17. By sorting the data, a three-dimensional diagram of the radon concentration of the system is drawn as shown in Fig. 7. Figure 7 is divided into two layers: the upper layer is the three-dimensional diagram of the radon concentration, and the lower layer is the plane diagram of the radon concentration anomaly. The scope of the fire

area was delimited based on the basic principle that the median radon concentration was greater than 3 times that of the fire source point, and the range of the median radon concentration was greater than 2 times that of the fire source (Liu and Wang 2017). The scope was delimited in the plan for the abnormal radon concentration in Figs. 6, and 7 areas of abnormal radon concentration were obtained, namely, A, B, C, D, E, and F; the abnormal areas cover an area of 54,500 m<sup>2</sup>, including two surface fires detected by infrared thermal imaging.

2. Drilling and temperature measurement verification

The radon release value in the formation is affected not only by the high-temperature condition but also by the influence of geological conditions, such as the aquifer, fault, and lithology. Therefore, to further verify whether the above abnormal radon

**Fig. 7** Radon concentration distribution. The upper layer is a three-dimensional diagram of the radon concentration, while the lower layer is a plane diagram of the radon concentration anomaly. The red circle in the figure is the delineated area of the radon concentration anomaly

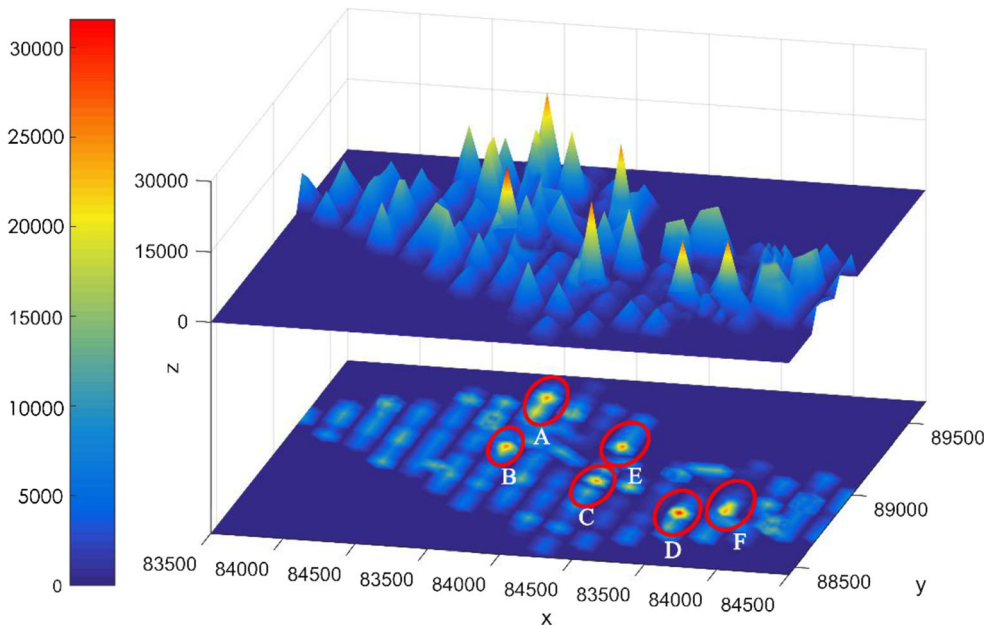
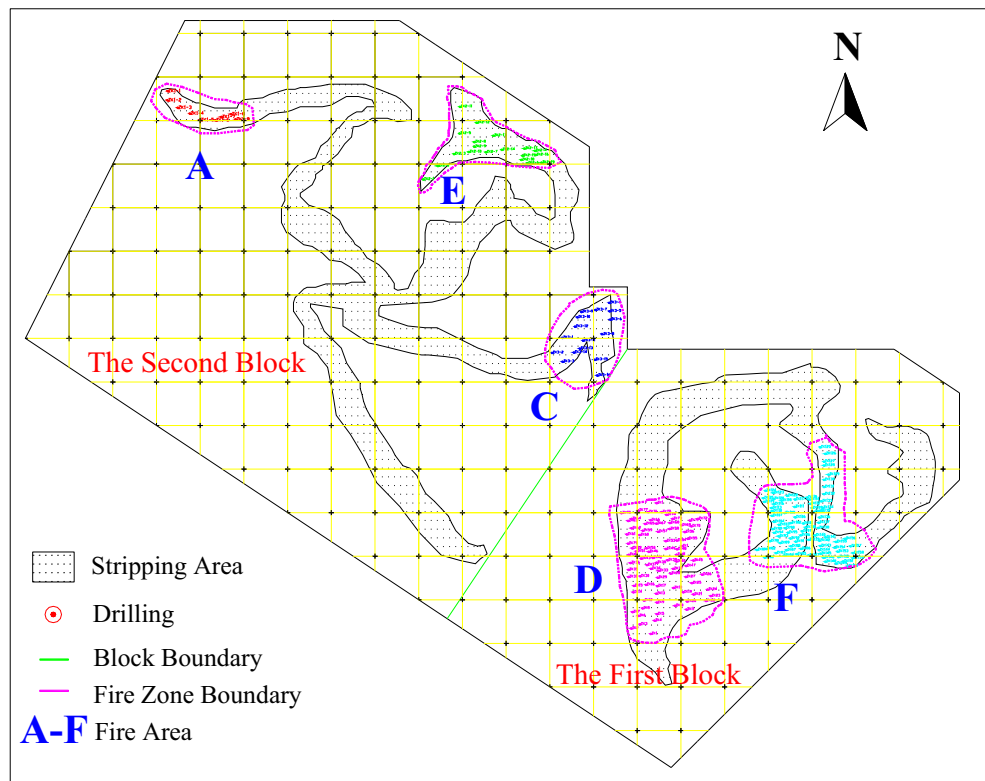


**Fig. 8** Distribution of fire area and drilling operations. The fire area is divided into two parts: the first section contains the D and F fire areas, and the second section includes the (A), (C), and (E) fire areas. The shaded part is the excavation route and road construction



value regions of A, B, C, and D (2 surface fires were validated by infrared thermal imaging) are high-temperature fire source points, drilling was carried out on the surface corresponding to the geometric center of the abnormal radon value region using a drilling machine. The geometric center of the radon anomaly areas corresponded to the surface through which the drill hole was constructed. A Hz-130y drilling machine is adopted to create drill holes with a hole diameter of 108 mm and a final

hole diameter of 89 mm. After drilling, the bottom temperature of the drilling hole is measured by an armored thermocouple, and the four regions A, B, C, and D have measured temperatures of 120 °C, 19 °C, 128 °C, and 123 °C, respectively. The borehole temperatures in the A, C, and D regions are all over 120 °C; thus, these areas belong to the high-temperature abnormality areas, which can be determined as a coal fire area; the B area temperature is 19 °C, and the drilling borehole temperature

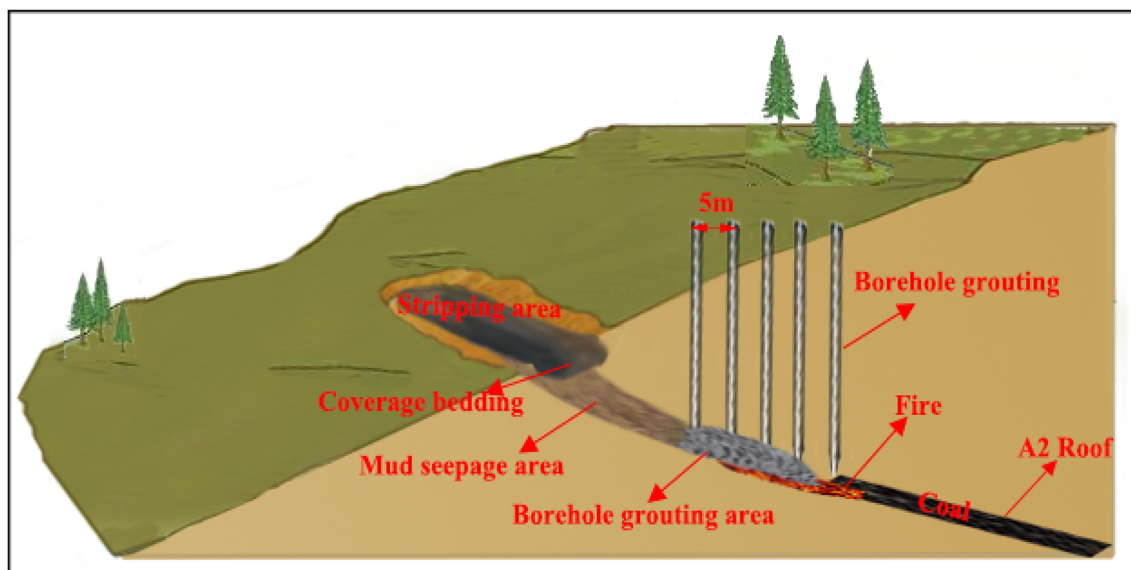
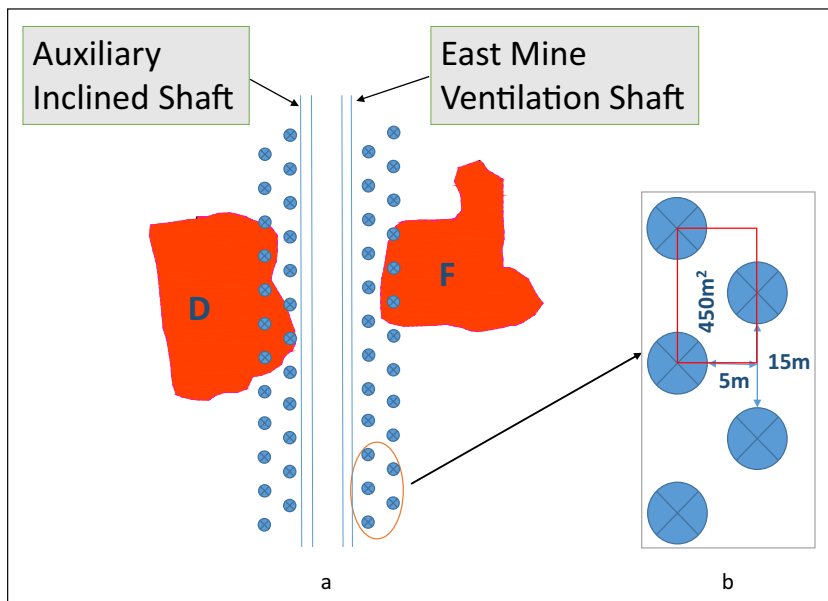


**Fig. 9** Schematic diagram of outcrop coal fire control



**Fig. 10** Drill hole layout for isolation construction in a fire area



is the same as the original rock formation temperature. The borehole depth in the center of region B is 121.8 m, and a solid coal seam with a thickness of 3.4 m appears at a hole depth of 91.4 m. A second layer of coal appears at 110.8 m. When drilling with the drilling rig, there is no burning phenomenon in either layers of coal. During the drilling process, intermittent slurry leakage occurred in the borehole, which was extremely serious and indicated that there were a large number of primary fractures in the formation.

By comparing the two methods of radon and borehole temperature measurements in region B, it is found that the radon values in region B undergo a certain abnormal phenomenon. The highest radon value reached 24,803.58 Bq/m<sup>3</sup>, but due to radon exhalation, this value is affected not only by temperature but also by the lithology, fault, fissure zone, and aquifer geological conditions. There are many fractures in the original rock strata in this area (this can be proven by the large amount of leakage in the drilling process), and the B area is on the back of a steep cliff. These factors could lead to the values of radon anomalies in fire area B. Therefore, it can be judged that

the high temperature in region B is not caused by coal fire, and thus, it is not necessary to put out the fire.

The fire area of the No. 1 well in the Fukang mining area was detected and verified using infrared thermal imaging, isotope radon measurements, and borehole temperature measurements. A total of 5 fire areas were found, and the areas of each fire area were A-2073.9 m<sup>2</sup>, C-8209.9 m<sup>2</sup>, D-15,046.2 m<sup>2</sup>, E-7286.1 m<sup>2</sup>, and F-14,256.7 m<sup>2</sup>. The location of each fire area is shown in Fig. 8.

### Subsurface fire control

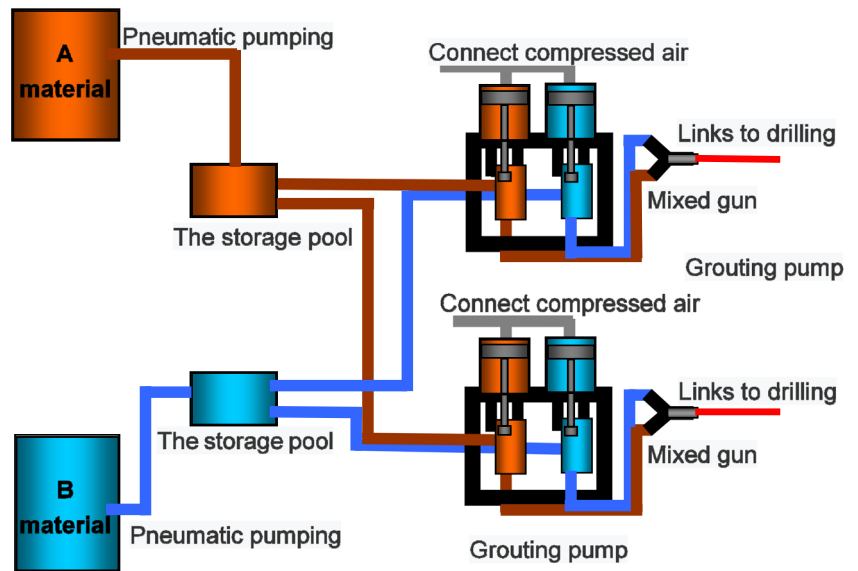
#### Detachment of shallow open flames

Surface stripping mainly includes two stripping steps and leveling of the mine fire area, the outcrop fire area and the concealed fire area. For outcrop coal fires on the west side of the E fire area and on the east side of the F fire area, the governance diagram is shown in Fig. 9. During the process

**Table 1** Amount of stripping and number of drilling sites in each fire area

Fire area number	Stripping range	Number of drilling sites	Stripping volume (m <sup>3</sup> )
A	Transportation road leveling and drilling platform	9	1900
C	Transportation road leveling and drilling platform	16	2500
D	Transportation road leveling and drilling platform	79	6900
E	Construction platform for outcrop fire stripping and drilling	19	3500
F	Construction platform for outcrop fire stripping and drilling	80	9400

**Fig. 11** Tiangu filling material production process



of outcrop fire detachment, due to the wide stripping of burning surfaces, the air leakage and oxygen supply conditions are sufficient in fire areas. To prevent fire deterioration caused by fire detachment, grouting isolation is first carried out in the outcrop deep fire zone boundary before fire detachment, thus preventing the fire from spreading deeper. Then, the loose outcrop coal fire is stripped, and the overburden is formed by grouting and loess coverage to reduce the air leakage and oxygen supply at the high-temperature fire source to extinguish the fire.

For the deep fire area with outcropping fire, grouting is carried out by surface drilling. The drilling hole diameter is 89 mm. In the formation fracture zone, casing is added to protect the wall. The grouting isolation boreholes are arranged in two rows in a tricornered pattern with a spacing of 5 m and 15 m, as shown in Fig. 10(b).

In the stripping project, in addition to stripping the fire areas E and F, the construction site and transportation route

of fire areas A, C, and D are leveled and stripped. The shaded part in Fig. 8 represents the stripping and leveling of roads in each fire area. By surveying and mapping the topography and landform of the fire area and comparing the changes in the topography and landform before and after excavation, the fire stripping volume is calculated and is shown in Table 1.

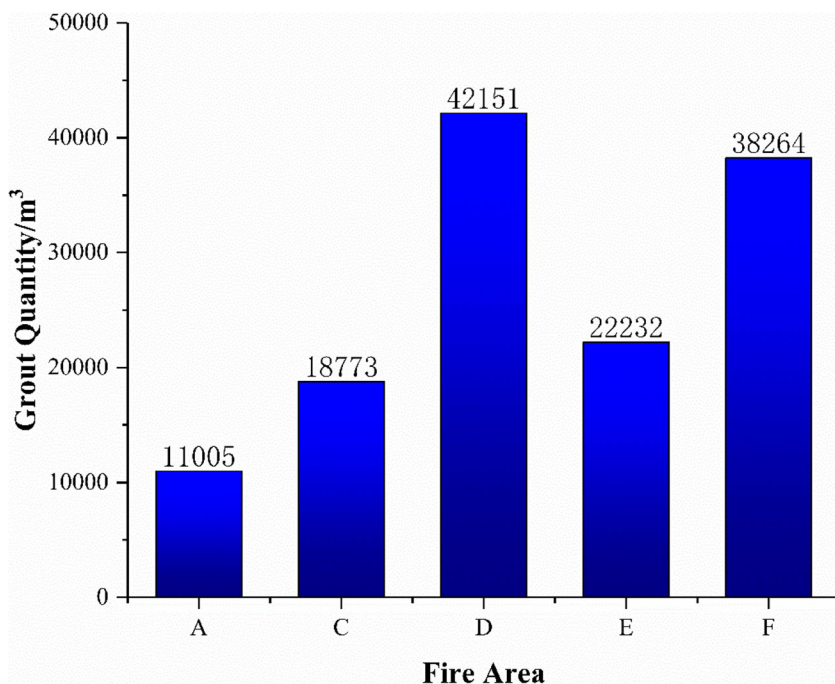
**Boundary isolation zone construction**

To strengthen the isolation effect on the fire area and prevent the depth of the fire area from extending to the goaf during the fire area treatment while reducing the influence of the fire areas D and F on the safety of the existing two shafts, as shown in Fig. 10(a), the auxiliary inclined shaft and east mine ventilation shaft are placed on either side of the border of the fire area to achieve dense drilling grouting isolation and a drilling depth to the A2 roof. The grouting isolation borehole is arranged in two rows in a tricornered pattern, with a spacing

**Fig. 12** Field foaming and stacking tests of Tiangu filling material



**Fig. 13** The amount of grout in each fire area



of 5 m and 15 m. The effective range of single-hole grouting is 450 m<sup>2</sup>, as shown in Fig. 10(b).

During the drilling construction process, some goaf cavities are larger where the goaf span height difference is more than 10 m. Therefore, Tiangu filling material for large-space bottom filling is first used in some goaf holes, and then plastic sodium silicate gel is used to fill in the gaps. Tiangu filling material is a polyurethane material with a high foaming rate that is especially used in underground coal mines. This material is mixed with A and B liquids in a ratio of 1:4, and the

foaming multiple is 25–30. This combination has better fire resistance, better high-temperature resistance, a higher foaming ratio, and better gas barrier performance than other materials. The filling materials must be mixed in a stable ratio of 1:4 with a special pneumatic grouting pump. When the pneumatic grouting pump is in use, the two feed pipes of the pump are inserted into the A and B barrels, as shown in Fig. 11. The air is slowly fed to the grout through the connected pressure fan, and the feed liquid enters the pump body from the two feed pipes. The mixture is fully mixed in the mixing



**Fig. 14** Water column produced during grouting (due to the high temperature in the borehole, part of the slurry rapidly vaporizes, resulting in slurry jetting out of the borehole and forming a 10-m-high water column)

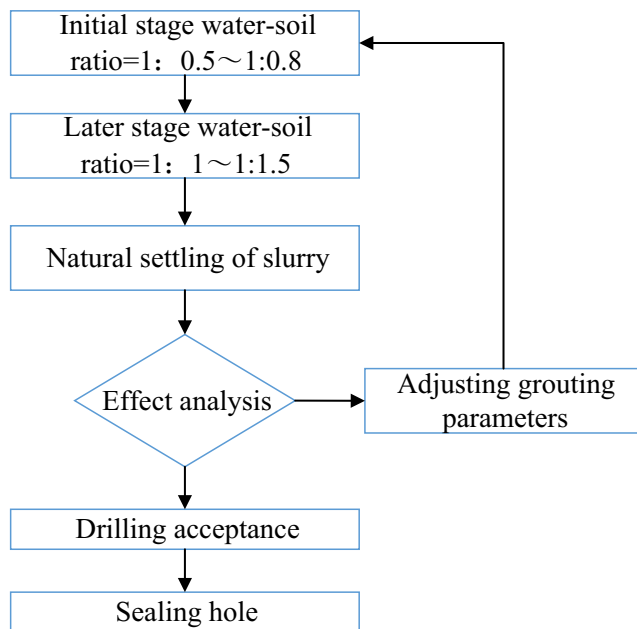


**Fig. 15** Flow chart of the grouting process

**Fig. 16** Stripping construction site: (a) plastic sodium silicate gel almost filled the entire goaf, and (b) the height of the water-glass gel stack can reach the top of the A2 coal seam



gun and injected into the target drilling hole position through the nozzle, as shown in Fig. 12. A total of 30 t of Tiangu filling material and 832,647 m<sup>3</sup> of plastic sodium silicate gel were used during the isolation zone construction project.

**Drilling and grouting in the deep fire area**

The grouting operation adopts the principle of controlling the deep fire source first and the shallow fire source later. The purpose is to control the deep fire source to prevent the shallow fire source that has just been controlled from being ignited by the heat generated by the high-temperature gases and the deep fire source. According to the overall technical scheme of the fire area management and the actual situation of the site, drilling and grouting were carried out in 5 fire areas. The positions of the drilling holes in each fire area are shown in Fig. 8, which shows that the fire areas D and F in the east have relatively dense boreholes. The fire area is generally strong in the east and weak in the west. A total of 203 boreholes were arranged throughout the entire fire area. The maximum borehole depth was 121.8 m, the minimum depth was 11.5 m, the average depth was 55.04 m, and the total footage of the boreholes was 11,175.4 m. The amount of grouting in each fire area is shown in Fig. 13. The grouting amount in fire areas D and F is more than that in fire areas A, C, and E. While the

burning in fire area D is more intense and the goaf cavity is larger, the construction of a separation wall in fire areas D and F requires more grout. Since most of the D and F fire areas are in the area of serious fire, surface collapse results in higher borehole temperatures, high temperatures in the deep strata result in rock breakage, a large amount of steam is produced during drilling, and the drilling temperature reaches approximately 500 °C. During grouting construction and the grouting process, due to the high temperature in the borehole, part of the slurry rapidly vaporizes, resulting in the slurry jetting out of the borehole and forming a 10-m-high water column, as shown in Fig. 14.

Plastic sodium silicate gel is a commonly used inorganic gel for preventing spontaneous coal combustion. When injected into loose media, sodium silicate gel can fill the coal seam body, evaporate, absorb heat, prevent air leakage, and isolate air, thus effectively preventing and extinguishing spontaneous coal combustion fires (Wang et al. 2016). During grouting construction, the grouting parameters are optimized until reaching the desired grouting effect. The grouting process is shown in Fig. 15. (1) At the beginning of the grouting process, the soil and water ratio is 1:0.5~1:0.8 to ensure that the borehole permeability and effective diffusion radius of the slurry increase the loess or the proportion of fly ash; to strengthen the mined-out area in the late grouting fissure

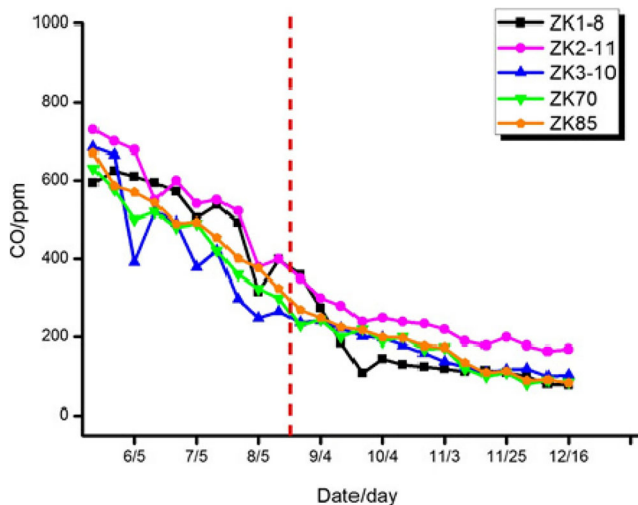


**Fig. 17** Temperature change in the test hole (the dotted red line is the construction completion date)

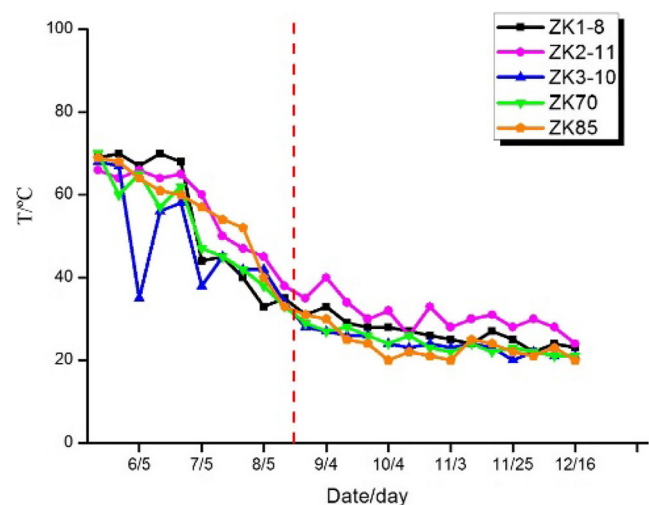
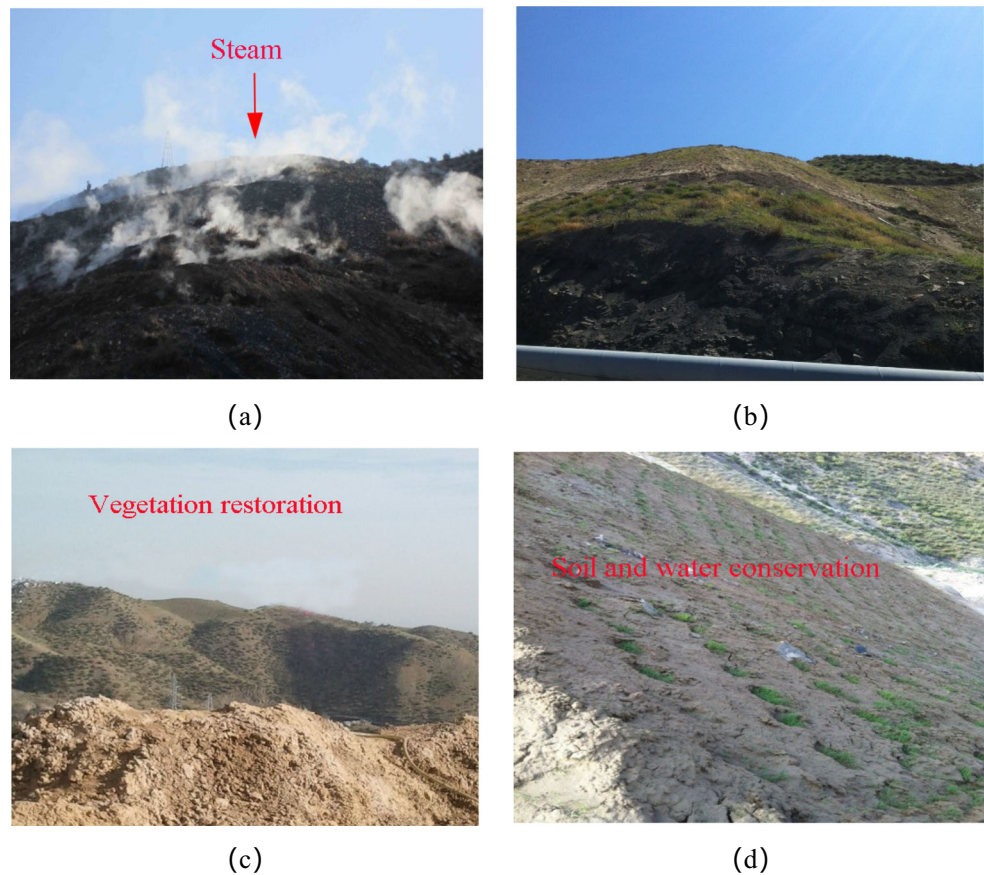


**Fig. 18** Variation in the CO concentration in the observation hole (the dotted red line is the construction completion date)

**Fig. 19** Comparison before and after the firefighting measures. (a) and (b) are a comparison of the surface conditions in the No. 1 fire area before and after grouting; (c) and (d) are restorations of vegetation on the surface after the completion of construction



sealing process, the soil and water ratio is adjusted to 1:1~1:1.5. (2) To prevent the grouting pipe from being blocked and simultaneously enhance the water-retaining and moisturizing effects of the yellow mud, a certain amount of JJJ-1 colloidal firefighting material should be added during the grouting process. The mass ratio of water and JJJ-1 colloidal material is 1:0.2%. (3) During the grouting process, multiwheel interval grouting is adopted. The amount of grouting for each hole is approximately  $100\text{ m}^3$  to ensure the natural precipitation and diffusion radius of the slurry. (4) The grouting construction for each hole is completed when the outlet pressure of the grouting pump shows an upward trend and exceeds 1.0 MPa.

## Long-term observations on the subsurface fire status and ground vegetation

### Isolation stripping

Stripping was carried out at a distance of approximately 50 m on the west side of the F fire isolation zone, and the stripping construction site is shown in Fig. 16. As seen in Fig. 16, the plastic sodium silicate gel was poured into the grouting area of

the isolated borehole, almost filling the entire goaf; all coal pillars were covered by plastic sodium silicate gel material, and the roadway in the goaf was also filled. The plastic water-glass gel trace left by the coal pillar shows that the isolated grouting technique can completely fill the chamber and pillar goaf.

### Observation hole for verification

After the construction process was complete, one borehole was reserved in the central area of each fire area as a test hole, and the gas temperature and CO concentration in the borehole were monitored and analyzed regularly. From May 15, 2011, to December 16, 2011, a total of 4 monitoring boreholes were continuously tested for 7 months; the monitoring data before August 20 were obtained during grouting, and the continuous observation data were obtained after August 20, as shown in Figs. 17 and 18. As shown in Fig. 17, during the grouting stage and with the progression of grouting, the drilling temperature decreases gradually and rapidly. After the grouting project, the drilling temperature stabilizes in the region. As shown in Fig. 18, the CO concentration decreases rapidly during the grouting stage and slowly drops after grouting until the final concentration is lower than 200 ppm. The

temperature and CO concentration data from the monitoring borehole indicate that the open fire in the fire area was extinguished.

Within 4 months after grouting, there was no sharp rise in temperature, and the drilling temperature tended toward a normal temperature. From the field, the surface combustion characteristics basically disappeared, and vegetation restoration occurred on the surface, as shown in Fig. 19.

In the past 3 years, a series of measurements, including stripping, drilling, and grouting, were taken in the fire area, and obvious effects were achieved by treating the fire area. There was no water vapor on the surface and no high temperatures in the drilling hole. To ensure the integrity of the project, loess was used to cover the fire area, and vegetation restoration occurred in July 2013.

## Conclusion

In the past 2 years, a variety of combined detection and fire extinguishing methods were carried out in fire areas, and remarkable effects were achieved in fire area management. No high temperatures were observed in the boreholes, and no water vapor was observed on the surface. This project provides a new method for coal mine fire control and has broad application prospects. The methods and results are summarized as follows:

1. The comprehensive detection range method was used for detecting the fire area, and a shallow outcrop fire was detected by infrared thermal imaging; the underground concealed fire source was detected by using the isotopic radon measurements, thus delineating the radon anomalies; the temperature verification of abnormal radon areas was carried out by means of borehole temperature measurements, and a total of 5 large fire areas were detected.
2. According to the characteristics of the large complex coal fire area in the mine, a zonal fire extinguishing scheme, namely, the “shallow open fire stripping—construction of the boundary isolation zone—drilling and grouting in the deep fire area” scheme, was designed and applied. After the completion of construction, the fire extinguishing effect was tested; the temperature in the fire area cooled in a short time, and no subsequent heating phenomenon occurred.
3. A new type of water-glass gel filling material and an automatic grouting system were developed. The self-developed automatic filling system was adopted for this process to realize surface channel conveyance and conveyance of slurry pump pipeline materials and to optimize the grouting parameters according to the grouting effects. In the initial stage, the permeability of the borehole and the effective diffusion radius of the slurry can be

guaranteed. In the middle stage, adjustments to the material properties are needed, along with strengthening of the water-retention effects and moisturizing effects of yellow mud, and prevention of pipeline blockage. In the later stage, multiwheel interval grouting can ensure the natural precipitation and diffusion radius of the slurry. Grouting construction of a hole is complete when the pump pressure exceeds 1.0 MPa.

The fire area in well No. 1 was successfully extinguished using the zonal fire extinguishing scheme and the dynamic grouting system, which shows that the scheme is feasible for large-scale complex coal fire extinguishing projects. The method proposed in this paper provides guidance and a reference for other coal fires in the world.

**Acknowledgments** We appreciate the editor’s efforts and those of the anonymous reviewers who provided valuable comments and suggestions for our research.

**Funding information** This work was financially supported by the National Key Research and Development Program of China (2016YFC0801800) and the Beijing Natural Science Foundation (2174084), as well as the National Nature Science Foundation of China (51774291, 51864045).

## References

- BP (2018) (2018) BP Statistical Review of World Energy
- Cao D, Shi X (2009) Comprehensive evaluation index system and evaluation method of environmental impact in coal field and fire area. *J Earth Sci Environ* 31:94–99
- Dai S, Ren D, Chou CL, Finkelman RB, Seredin VV, Zhou Y (2012) Geochemistry of trace elements in Chinese coals: a review of abundances, genetic types, impacts on human health, and industrial utilization. *Int J Coal Geol* 94:3–21
- Dijk PV, Zhang J, Wang J, Kuenzer C, Wolf KH (2011) Assessment of the contribution of in-situ combustion of coal to greenhouse gas emission; based on a comparison of Chinese mining information to previous remote sensing estimates. *Int J Coal Geol* 86:108–119
- Finkelman RB (2004) Potential health impacts of burning coal beds and waste banks. *Int J Coal Geol* 59:19–24
- Kong B, Li Z, Yang Y, Liu Z, Yan D (2017) A review on the mechanism, risk evaluation, and prevention of coal spontaneous combustion in China. *Environ Sci Pollut Res* 24:1–18
- Kuenzer C, Stracher GB (2012) Geomorphology of coal seam fires. *Geomorphology* 138:209–222
- Kuenzer C, Zhang J, Tetzlaff A, van Dijk P, Voigt S, Mehl H, Wagner W (2007) Uncontrolled coal fires and their environmental impacts: investigating two arid mining regions in north-central China. *Appl Geogr* 27:42–62
- Li Z, Kong B, Wei A, Yang Y, Zhou Y, Zhang L (2016) Free radical reaction characteristics of coal low-temperature oxidation and its inhibition method. *Environ Sci Pollut Res* 23:23593–23605
- Liang Y, Liang H, Zhu S, Liang Y, Liang H, Zhu S (2014) Mercury emission from coal seam fire at Wuda, Inner Mongolia, China. *Atmos Environ* 83:176–184

- Liu Z, Wang W (2017) Application of instantaneous measurement of radon in the detection of hidden fire sources in small coal pits. *Coal Mine Saf* 48:148–154
- Liu W, Qin Y, Yang X, Wang W, Chen Y (2018) Early extinguishment of spontaneous combustion of coal underground by using dry-ice's rapid sublimation: a case study of application. *Fuel* 217:544–552
- Rúa MOB, Baena PB, Aragón AJD (2018) Optimization of techniques for the extinction and prevention of coal fires produced in final walls as a result of spontaneous combustion in the Cerrejón mine—Colombia. *Environ Sci Pollut Res* 25:32515–32523
- Shao Z, Wang D, Wang Y, Zhong X, Tang X, Hu X (2015) Controlling coal fires using the three-phase foam and water mist techniques in the Anjialing Open Pit Mine, China. *Nat Hazards* 75:1833–1852
- Shao Z, Jia X, Zhong X, Wang D, Wei J, Wang Y, Chen L (2018) Detection, extinguishing, and monitoring of a coal fire in Xinjiang, China. *Environ Sci Pollut Res* 25:26603–26616
- Song Z, Kuenzer C (2014) Coal fires in China over the last decade: a comprehensive review. *Int J Coal Geol* 133:72–99
- Song Z, Kuenzer C (2017) Spectral reflectance (400–2500 nm) properties of coals, adjacent sediments, metamorphic and pyrometamorphic rocks in coal-fire areas: a case study of Wuda coalfield and its surrounding areas, northern China. *Int J Coal Geol* 171:142–152
- Song Z, Zhu H, Bo T, Wang H, Qin X (2014) Numerical study on effects of air leakages from abandoned galleries on hill-side coal fires. *Fire Saf J* 69:99–110
- Song Z, Kuenzer C, Zhu H, Zhen Z, Jia Y, Sun Y, Zhang J (2015) Analysis of coal fire dynamics in the Wuda syncline impacted by fire-fighting activities based on in-situ observations and Landsat-8 remote sensing data. *Int J Coal Geol* 141–142:91–102
- Song Z, Wu D, Jiang J, Pan X (2019) Thermo-solutal buoyancy driven air flow through thermally decomposed thin porous media in a U-shaped channel: towards understanding persistent underground coal fires. *Appl Therm Eng* 159:113948
- Stracher GB (2004) Coal fires burning around the world: a global catastrophe. *Int J Coal Geol* 59:1–6
- Stracher GB, Prakash A, Sokol EV, Stracher GB, Prakash A, Sokol EV (2013) Preface to volume 1 - Coal and peat fires: a global perspective. *Coal & Peat Fires A Global Perspective*, pp vii–viii
- Wang K (2013). Experimental study on oxidative spontaneous combustion of Jurassic coal in northern Shanxi. Xi'an University of Science and Technology
- Wang K, Wei LU, Yunfeng DU, Zhang Q, Jun XU (2016) Study on plastic water glass gel for preventing coal spontaneous combustion. *Min Saf Environ Prot* 43:8–11
- Xue S, Dickson B, Wu J (2008) Application of Rn technique to locate subsurface coal heatings in Australian coal mines. *Int J Coal Geol* 74:139–144
- Zeng Q, Tiyyip T, Wuttke MW, Guan WM (2015) Modeling of the equivalent permeability for an underground coal fire zone, Xinjiang region, China. *Nat Hazards* 78:957–971
- Zhang J (2008) Research and control of underground coal fire in China. Coal industry Press

**Publisher's note** Springer Nature remains neutral with regard to jurisdictional claims in published maps and institutional affiliations.